

## OPTIMAL CONTROL STRUCTURE FOR VARIABLE SPEED WIND POWER SYSTEM

Nicolaos Antonio CUTULULIS, Iulian MUNTEANU, Emil CEANGA,  
Mihai CULEA

*"Dunărea de Jos" University of Galati, Romania*

**Abstract:** This paper presents an optimal control structure for variable speed, fixed pitch wind turbine. The control objective results from the optimization criterion that includes two contradictory demands: maximization of the energy captured from the wind and minimization of the damage caused by mechanical fatigue. We admit, as a modeling assumption, that wind speed has two components: a slowly varying component, named *seasonal* and a rapidly varying component, named *turbulence*. Hence, two control structures, which should function simultaneously, are identified in the optimal control problem.

The first optimization structure aims to maximize the wind turbine energetic efficiency by maintaining operational point on optimal regime characteristics (ORC). According to the slowly varying seasonal component of wind speed, a control loop adjusts system operating point in order to maintain it on ORC. In the second optimization structure, the system is considered to be operating on "static" optimal point assured by the above mentioned control loop, with the turbulence component being the input variable. The second control loop aims dynamic optimization that implies the minimization of the tip speed ratio variations around its optimal value, while minimizing the torque variations, thus the mechanical stress. Mathematically, this objective is defined as an integral criterion, belonging to linear quadratic optimization.

**Keywords:** wind power, variable speed operation, wind modelling, linear quadratic optimal control.

### 1. INTRODUCTION

The performances of the wind energy conversion systems decisively depend on the correct statement and the efficient solving of the associated control problem. The maximization of the energy conversion – in the sense of maximizing the power coefficient,  $C_p$  – has been the most used control goal for long time. Because the optimal value of this coefficient is obtained for a well-determined tip speed ratio,  $\lambda_{opt}$ , the optimal control was usually implemented by tracking the desired value of the shaft speed,  $\Omega^{ref} = \frac{v \cdot \lambda_{opt}}{R}$ . Recently, not only the energetic aspect is considered in defining the performance criterion, but also that of reliability. In order to reduce the mechanical fatigue of the drive train, it is

imposed the minimization of the torque variations, by controlling the generator torque variations,  $\Delta\Gamma(t)$ . In (Ekelund, 1997), the antagonist demands of maximizing the energy conversion and minimizing the torque variations are expressed by a combined optimization criterion:

$$(1) J = E \left\{ \alpha \cdot [\lambda(t) - \lambda_{opt}]^2 + \Delta\Gamma^2(t) \right\}$$

where  $E\{\cdot\}$  is the statistical average symbol. If only the first component from (1) is minimized, the functioning around the optimal regime is ensured, but with the price of some important torque variations. The trade-off between these two requirements can be adjusted by the ponderation coefficient  $\alpha$ .

The Gaussian linear quadratic problem was solved by using an adaptive control structure (Ekelund 1997),

as the dynamical system's parameters depend on the operating point chosen on the turbine's characteristic, and this latter depends on the average wind speed.

In this paper, a new optimal control structure is proposed, which optimizes the combined integral criterion without using adaptive structures. The basic principle used relies upon separating the turbulence and the seasonal (low frequency) wind speed components (Nichita, *et al*, 2001). The two components act separately within two loops of the proposed control structure. Thus, the low frequency component generates the input of the shaft speed control loop, ensuring to reach the "static" optimal operating point on the  $C_p(\lambda)$  characteristic. The turbulence component acts within an optimal control loop, having as performance criterion the one given in relation (1), but in deterministic approach.

The paper is organized as follows. In the next section is presented the modeling of the wind as a non-stationary stochastic process and the separation of the two components above mentioned. Section 3 presents the control system structure in relation with the seasonal wind speed component, as well as the model of the system around the optimal point ensured by the low frequency control loop. It is proved that this system is invariant. The optimal control law depending on the turbulence component is designed in Section 4. In the Section 5, some simulation results are presented. The concluding remarks end this paper.

## 2. WIND SPEED MODELING

The wind speed is considered as consisting of two elements:

- a slowly varying mean wind speed of hourly average. Usually, this component is modelled as a Rayleigh distribution (Leithead, *et al*, 1991):

$$(2) p_R = (\bar{v}) = a \cdot v \cdot e^{-1/2a\bar{v}^2}$$

where  $\bar{v}$  is the hourly wind speed average and  $a$  is related to the very long time scale mean speed;

- a rapidly varying turbulence component, modelled by a normal distribution with mean value equal to zero and standard deviation proportional to the current value of the average wind speed. The dynamic properties of the turbulence component are given by the Von Karman power spectrum:

$$(3) S_{vv}(\omega) = \frac{0.475\sigma^2 L/\bar{v}}{\left[1 + (\omega L/\bar{v})^2\right]^{5/6}}$$

where  $\sigma$  is the turbulence intensity and  $L$  is the turbulence length scale.

## 2.1. VAN DER HOVEN'S LARGE BAND MODEL OF THE WIND SPEED

In studies concerning the hybrid Wind-Diesel systems, a reference model for the wind speed is considered the Van der Hoven's experimental model (Lipman, 1990), reproduced in Figure 1. The power spectrum of the horizontal wind speed is calculated in the range from 0.0007 to 900 cycles/hour, which is more than six decades. The knowledge of the spectral characteristic of the wind speed in such a frequency range would bring solutions to wind simulation research, as it contains the spectral domain that describes the medium and long-term variations, as well as the spectral range of the turbulence component.

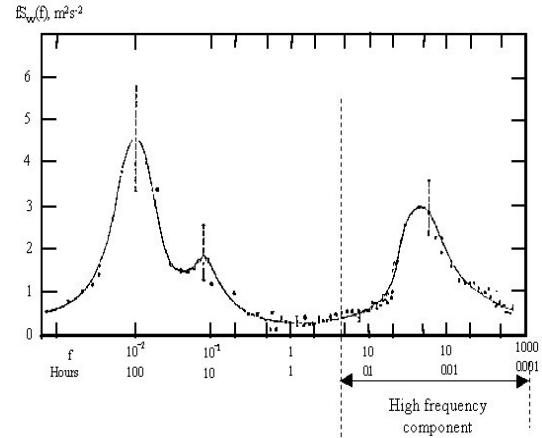


Fig.1. Van der Hoven's spectral model

Starting from an experimental characteristic, the numerical procedure used for the wind speed generation is based on the sampling of the spectrum.

We can also remark that the turbulence component in the Van der Hoven model is a stationary stochastic system.

Let us consider  $\omega_i, i = \overline{1, N+1}$ , the discrete angular frequency and  $S_{vv}(\omega_i)$  the corresponding values of the power spectral density. The harmonic at the frequency  $\omega_i$  has the amplitude

$$(4) A_i = \frac{2}{\pi} \sqrt{\frac{1}{2} [S_{vv}(\omega_i) + S_{vv}(\omega_{i+1})] \cdot [\omega_{i+1} - \omega_i]}$$

and the phase,  $\varphi_i$ , randomly generated. The wind speed,  $v(t)$ , is simulated by the relation

$$(5) v(t) = \sum_{i=0}^N A_i \cos(\omega_i t + \varphi_i)$$

where  $\omega_0 = 0, \varphi_0 = 0$  and  $A_0 = \bar{v}$  is the mean wind speed, calculated on a time horizon greater than the

largest period in Van der Hoven's characteristic (i.e.,  $T = 2\pi/\omega_1$ ).

## 2.2. VON KARMAN'S MODEL OF THE TURBULENCE COMPONENT

Experimental data show that the turbulence component characteristic depends on the value of the mean speed. (Welfonder, *et al.*, 1997) deals with a simulation scheme, where the non-stationary turbulence component is modelled using a shaping filter, which colours a synthetically produced white noise. The transfer function of the shaping filter, according to the von Karman's turbulence spectrum (Welfonder, *et al.*, 1997; Ekelund, *et al.*, Leithead, *et al.*, 1991) is:

$$(6) H_F(j\omega) = \frac{K_F}{(1 + j\omega T_F)^{5/6}}$$

where the  $K_F$  and  $T_F$  parameters depends on the medium speed of the wind.

## 2.3. LARGE BAND MODELLING OF THE WIND SPEED

The solutions used hereafter are based on the following remarks, issued from the previous sections (Nichita, *et al.*, 2001):

- the method based exclusively on the Van der Hoven model leads to incorrect results, as the turbulence component is not modeled as a non-stationary process;
- the procedure used in (Welfonder, *et al.*, 1991), based on the von Karman spectrum, can model the turbulence component as a non-stationary process, but doesn't reproduce the slow fluctuations, that correspond to the low frequency domain in the spectral characteristic of the wind speed.

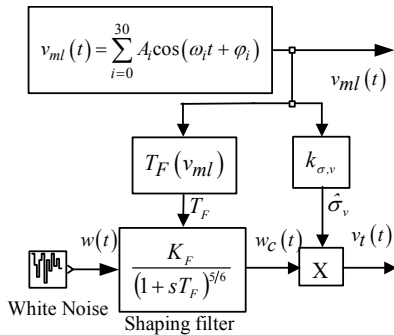


Fig.2. Non-stationary wind speed generation

Consequently, we combine the low frequency model of Van de Hoven's characteristic with a non-stationary turbulence model. We made the assumption that the discrete frequency values  $f_0=0$ ,

$f_1=0.001$  cycles/h,..., $f_{30}=4$  cycles/h correspond to the spectral range that describes medium and long term wind speed evolution and the turbulence component (i.e. the short-term component) is given by the spectral range between 5 cycles/hour and 1000 cycles/hour, that corresponds to frequencies  $f_{31}, \dots, f_N$ , with  $N=55$ . In this case,  $v(t)$  becomes,

$$(7) v(t) = v_{ml}(t) + v_t(t)$$

where

$$(8) v_{ml}(t) = \sum_{i=0}^{30} A_i \cos(\omega_i t + \varphi_i)$$

is the medium and long term component and  $v_t(t)$  is the turbulence component. We have considered that Van de Hoven's model describes correctly only the wind variation on a large time scale, so  $v_{ml}(t)$  will be used in the final wind model.

The high frequency model is presented in Fig. 2 (Welfonder, *et al.*, 1991), (Nichita, *et al.*, 2001) in which has been noted:

$k_{\sigma,v}$  – the shape of the regression curve that statistically describes the relation between the mean value  $v_{ml}$  and the standard deviation  $\hat{\sigma}_v$ ;

$T_F$  – the time constant of the filter and is dependent of the  $v_{ml}$ :  $T_F = \frac{L}{v_{ml}}$  and  $L$  is the turbulence length scale;

$K$  – the static gain obtained from the condition that the variance of the coloured noise  $w_c(t)$  is equal to 1:

$$K \cong \sqrt{\frac{2 \cdot \pi \cdot T_F}{B \left( \frac{1}{2}, \frac{1}{3} \right) T_s}} \text{ where } B \text{ designates the beta}$$

function and  $T_s$  is sampled period.

## 3. LOW FREQUENCY SYSTEM STRUCTURE

The structure of the system that assures optimal conversion regime, according to the medium and long term component of the wind speed, is presented in Fig. 3.

There, the block named  $F$  is an fourth order Butterworth filter, which extracts the slowly varying component  $v_{ml}(t) \equiv \bar{v}(t)$ , from the wind speed,  $v(t)$ .

According to this variable, the optimal reference  $\bar{\Omega}^{opt}(t)$  is generated, in a shaft's speed control loop.

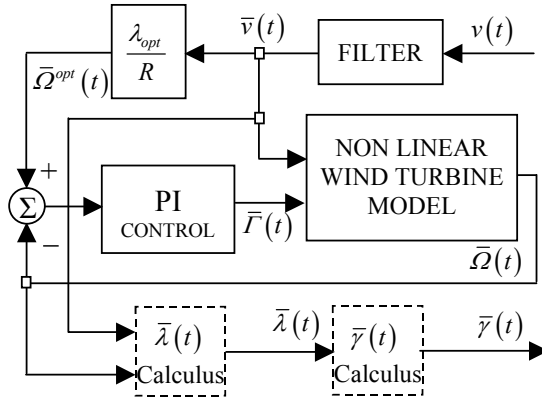


Fig.3. Low frequency system structure

This is accomplished using the electrical generator's load system (Fig. 4). The controlled generator torque

$\Gamma(t)$  has two components:  $\bar{\Gamma}(t)$  generated by the low frequency loop PI controller and  $\Delta\Gamma(t)$  according to the wind speed turbulence component, generated by the optimal LQ controller (see Section 5).

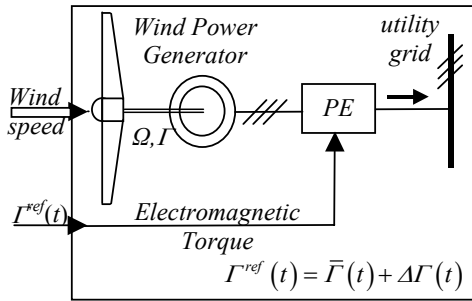


Fig.4. Electrical generator's load system

The non – linear wind generator model is given by the movement equation:

$$(9) J \frac{d\Omega}{dt} = \Gamma_e(\Omega, v) - \Gamma$$

where the wind torque is:

$$(10) \Gamma_e = \frac{1}{2} \rho \pi R^2 v^3 \frac{C_p(\lambda)}{\Omega}$$

and  $J$  is the drive train inertia.

We linearise the model around an operating point:

$$(11) \Delta\Gamma_e = \frac{\partial\Gamma_e}{\partial\Omega} \Delta\Omega + \frac{\partial\Gamma_e}{\partial v} \Delta v$$

$$(12) \frac{\partial\Gamma_e}{\partial\Omega} = \frac{1}{2} \rho \pi \frac{R^2 v^3}{\Omega^2} [C'_p(\lambda)\lambda - C_p(\lambda)]$$

$$(13) \frac{\partial\Gamma_e}{\partial v} = \frac{1}{2} \rho \pi \frac{R^2 v^2}{\Omega} [3C_p(\lambda) - \lambda C'_p(\lambda)]$$

After normalizing the variables involved, the linearised model of the wind turbine is:

$$(14) \Delta\bar{\Gamma}_e = \gamma \cdot \Delta\bar{\Omega} + (2 - \gamma) \cdot \Delta\bar{v}$$

where  $\Delta\bar{\Gamma}_e = \Delta\Gamma_e / \bar{\Gamma}_e$ ;  $\Delta\bar{\Omega} = \Delta\Omega / \bar{\Omega}$ ;  $\Delta\bar{v} = \Delta v / \bar{v}$

$$(15) \gamma = \left[ \frac{\bar{\lambda} C'_p(\bar{\lambda}) - C_p(\bar{\lambda})}{C_p(\bar{\lambda})} \right]$$

We notice that model's parameters are relied on the variable  $\gamma$ , which depends directly on the tip speed ratio  $\lambda$ . The low frequency loop aims to maintain the tip speed ratio to its optimal value,  $\lambda_{opt} = 7$ . Due to the inherent dynamic errors of the loop, the variable  $\gamma$  will have small variations around a constant value. Thus, the wind system, which represents the fixed part of the high frequency optimal system, is practically time invariant (see numerical validation results in Section 5). Consequently, the high frequency optimal control does not involve an adaptive strategy.

#### 4. OPTIMAL CONTROL STRUCTURE

We consider the controlled system

$$(16) \begin{cases} \dot{\underline{x}}(t) = A\underline{x}(t) + B\underline{u}(t) + \underline{v}(t) \\ \underline{y}(t) = C\underline{x}(t); \end{cases}$$

where  $\underline{v}(t)$  is a measurable disturbance.

The imposed performance criterion has the general form below:

$$I = \frac{1}{2} \int_{t_0}^{\infty} \{ \underline{y}(t)^T S \underline{y}(t) + \underline{u}^T(t) R \underline{u}(t) \} dt$$

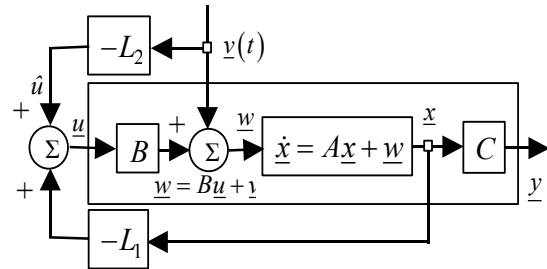


Fig.5. Optimal control system structure

The optimal control law is assured by the matrix coefficients  $L_1$  and  $L_2$ , presented in Fig. 5 which are

determined from the following Riccati equation (Athans, M. and Falb, P., 1966)

$$(17) PBR^{-1}B^T P - A^T P - PA - Q = 0$$

and the associated equation

$$(18) \left( A^T - PBR^{-1}B^T \right) p + P\underline{v} = 0$$

where  $Q = C^T SC$ .

The expressions of the above mentioned coefficients:

$$(19) L_1 = R^{-1}B^T P$$

$$(20) L_2 = -R^{-1}B^T \left( A^T - PBR^{-1}B^T \right)^{-1} p$$

Our optimized system has the state equation

$$(21) \dot{x} = \frac{\gamma}{J_T} x + \frac{2-\gamma}{J_T} \overline{\Delta v} - \frac{1}{J_T} u$$

where  $J_T = J \frac{\overline{\Omega}}{\overline{F}}$  is the total inertia of the linearized system. With the following notations:

$$(22) v = \frac{2-\gamma}{J_T} \overline{\Delta v}; \quad a = \frac{\gamma}{J_T}; \quad b = -\frac{1}{J_T}$$

the system becomes:

$$(23) \dot{x} = ax + bu + v$$

where  $x = \overline{\Delta\Omega}$ ;  $u = \overline{\Delta F}$ .

The combined performance criterion is

$$(24) I = \int_0^{\infty} \left[ \alpha \left( \lambda(t) - \lambda_{opt} \right)^2 + \Delta F^2(t) \right] dt$$

With

$$(25) \overline{\Delta\lambda}(t) = \overline{\Delta\Omega}(t) - \overline{\Delta v}(t)$$

after some elementary calculus, it becomes

$$(26) I = \int_0^{\infty} \left( \alpha x^2 - 2qx + u^2 \right) dt$$

where

$$(27) q(t) = -\alpha \frac{J_T}{2-\gamma} v(t)$$

Thus, we are dealing with a general LQ problem, with the following correspondences:

$$(28) A = a; \quad B = b; \quad Q = \alpha; \quad R = 1$$

The Riccati equation becomes:

$$(29) P^2 b^2 - 2aP - \alpha = 0$$

with the solution:

$$(30) P_{1,2} = J_T \left( \gamma \pm \sqrt{\gamma^2 + \alpha} \right)$$

The associated equation is:

$$(31) \left( a - Pb^2 \right) p + P\underline{v} - \alpha \frac{J_T}{2-\gamma} = 0$$

After some elementary calculus, we obtain the expressions of the coefficients  $L_1$  and  $L_2$ :

$$(32) L_1 = -\gamma \pm \sqrt{\gamma^2 + \alpha}$$

$$(33) L_2 = \frac{\left( \gamma \pm \sqrt{\gamma^2 + \alpha} \right) (2-\gamma) - \alpha}{\sqrt{\gamma^2 + \alpha}}$$

Therefore, the optimal control structure presented in Fig. 5, becomes (Fig. 6):

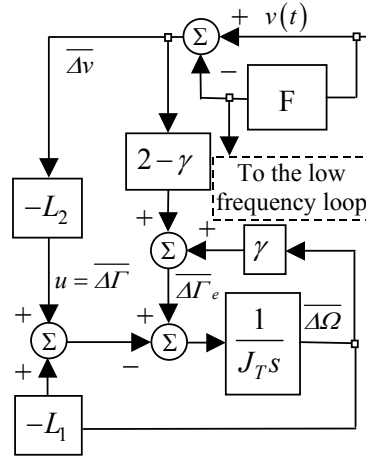


Fig.6. Optimal LQ control structure

## 5. SIMULATION RESULTS

In Fig. 7 are presented the results of the wind speed generation (a) using the model presented in Section 2, and the two components, the medium and long term component (b) and the turbulence component (c), obtained after filtering.

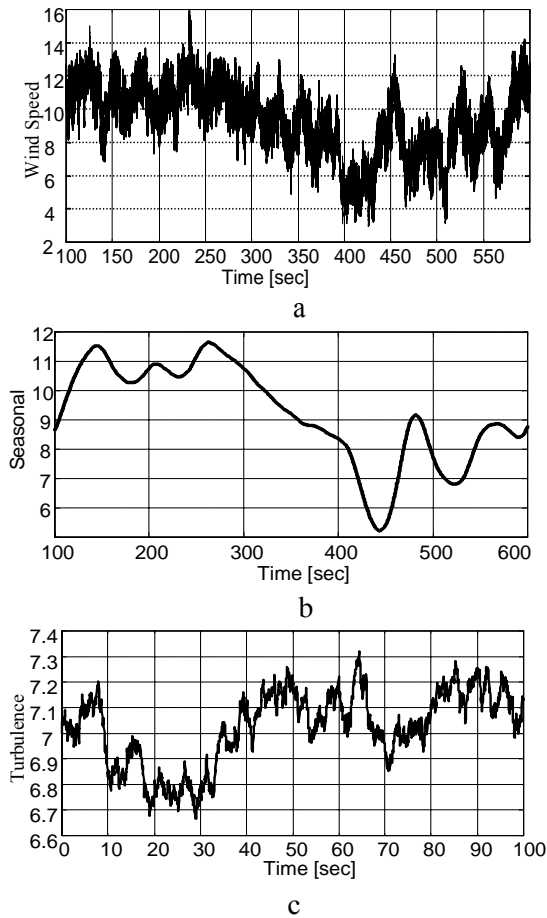


Fig.7. Wind speed (a), low frequency component (b) and turbulence component (c)

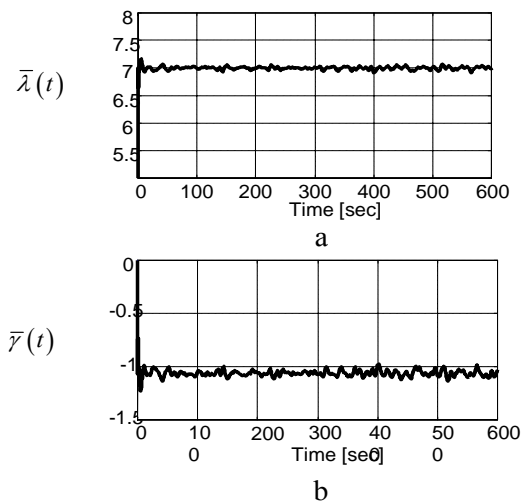


Fig.8. Variations of tip speed ratio  $\lambda$  (a) and of the  $\gamma$  coefficient (b)

The Fig. 8 presents the simulation results of the low frequency loop.

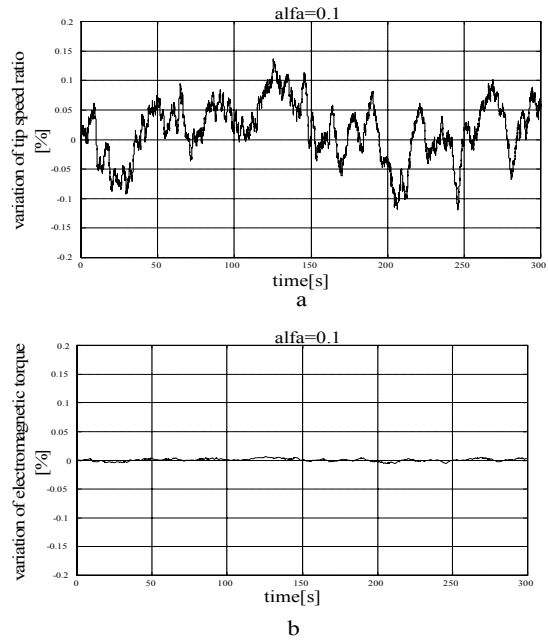


Fig.9. Variations of tip speed ratio (a) and electromagnetic torque (b) for  $\alpha = 0.1$

The first figure shows small variations of the tip speed ratio around its optimal value due to the variations of the medium and long term component of the wind speed. That implies small variations around the wind turbine's optimal functional point. This system will be optimized in the high frequency loop, improving the energetic efficiency of the wind power system and the compliance of its drive train.

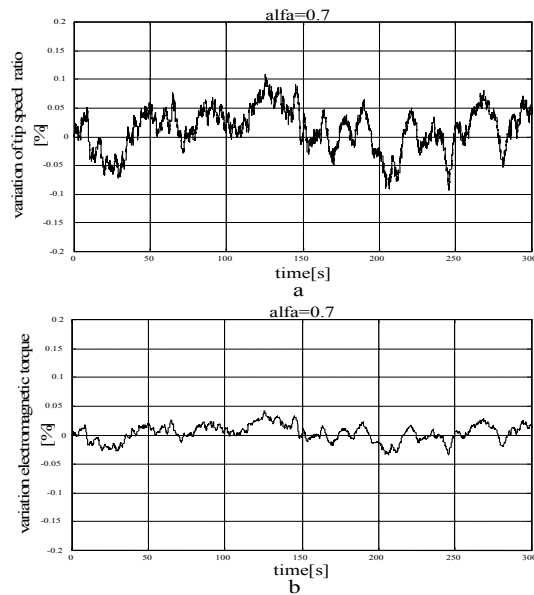


Fig.10. Variations of tip speed ratio (a) and electromagnetic torque (b) for  $\alpha = 0.7$

As shown in Section 3, parameter  $\gamma$  depends exclusively of the tip speed  $\lambda$ . Therefore, the low frequency loop will maintain  $\gamma$  practically time invariant, with small variations around a constant value (Fig. 7,b).

The combined performance criterion (24) shows that the trade-off between the energetic efficiency (minimization of  $\Delta\lambda(t)$ ) and mechanical stress (minimization of  $\Delta F(t)$ ) is realized by choosing the ponderation factor  $\alpha$ .

The Fig.9, 10, 11 and 12 permits a qualitative analysis of the optimization results and show how the variances of the tip speed ratio and electromagnetic torque depends on  $\alpha$ . The tip speed ratio variance increases with the value of  $\alpha$ , while the electromagnetic torque variance decreases.

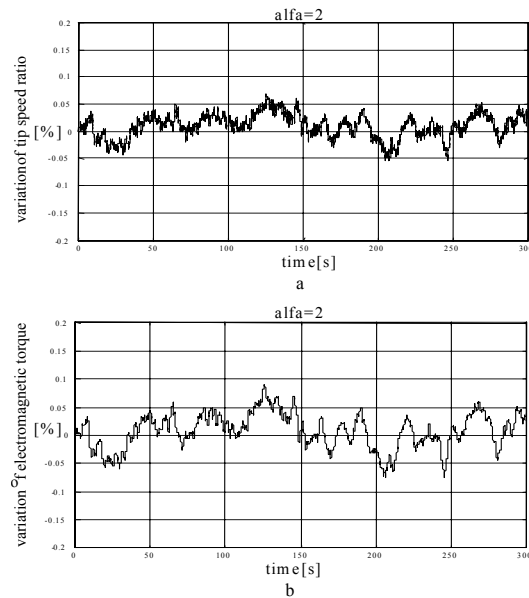


Fig.11. Variations of tip speed ratio (a) and electromagnetic torque (b) for  $\alpha = 2$

## 6. CONCLUDING REMARKS

The frequency separation principle adopted in the wind modeling has resulted in a particular configuration of the control structure – as an alternative to the adaptive structures – consisting of two different loops: the maximum energetic efficiency loop, governed by the low frequency wind speed component, and an optimal control loop, governed by the turbulence component. The optimality of the whole is defined in relation with the trade-off between energy conversion maximization and the control input minimization that determines the mechanical stress of the drive train. This optimal problem is treated within a complete linear quadratic deterministic approach, whose effectiveness was

proved by numerical simulation. Note the flexibility of the proposed control structure in relation with the type of the drive system used.

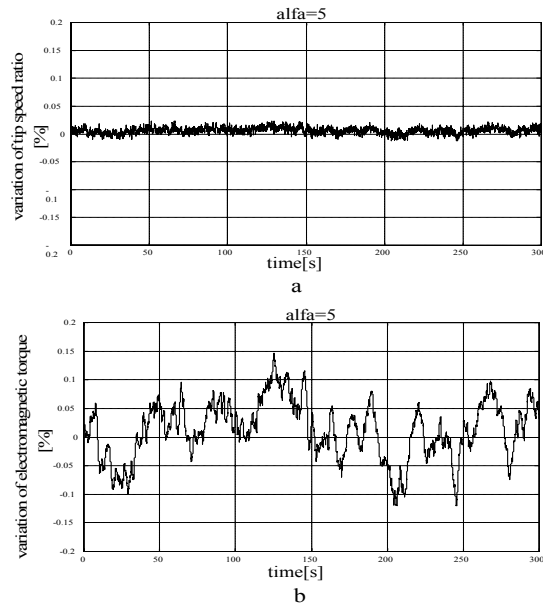


Fig.12. Variations of tip speed ratio (a) and electromagnetic torque (b) for  $\alpha = 5$

## 7. REFERENCES

- Ekelund, T. (1997). *Modeling and Linear Quadratic Optimal Control of Wind Turbines*, PhD Thesis, Chalmers University, Göteborg, Sweden.
- Leithead, W.E., de la SALE, S. and Reardon, D. (1991). *Role and objectives of Control For Wind Turbines*, IEEE Proceedings, **Vol. 138, No. 2**, pp. 135-148.
- Nichita, C., Luca, D., Dakyo, B., Ceanga, E., Cutululis, N.A. (2001). *Modeling non-stationary wind speed for renewable energy systems*, SIMSIS 11, Galati, Romania, pp. 289 – 294.
- Lipman, N.H. (1990). *Overview of wind/diesel systems*, Proceedings of the 1<sup>st</sup> World Renewable Energy Congress, **Vol. 3**, pp. 1547 – 1563, Reading, U.K.
- Welfonder, E., Neifer, R. and Spanner, M. (1997). *Development and Experimental Identification of Dynamic Models for Wind Turbines*, Control Engineering Practice, **Vol. 5, No. 1**, pp. 63 – 73.
- Van der Hoven, I. (1957). *Power Spectrum of horizontal Wind Speed in Frequency Range 0.0007 to 900 cycles per hour*. Journal of Metrology, **Vol. 14**, pp. 160 – 164.
- Athans, M., Falb, P. (1966). *Optimal Control*, McGraw – Hill, New York.